

The Aryl Hydrocarbon Receptor Modulates Production of Cytokines and Reactive Oxygen Species and Development of Myocarditis during *Trypanosoma cruzi* Infection

Andréia Barroso,^{a,b} Melisa Gualdrón-López,^b Lísia Esper,^{a,b} Fátima Brant,^{a,b} Ronan R. S. Araújo,^b Matheus B. H. Carneiro,^b Thiago V. Ávila,^{b,c} Danielle G. Souza,^c Leda Q. Vieira,^b Milene A. Rachid,^d Herbert B. Tanowitz,^e Mauro M. Teixeira,^{a,b} Fabiana S. Machado^{a,b}

Program in Health Sciences: Infectious Diseases and Tropical Medicine, Medical School,^a and Departments of Biochemistry and Immunology,^b Microbiology,^c and Pathology,^d Institute of Biological Sciences, Universidade Federal de Minas Gerais, Belo Horizonte, Brazil; Departments of Pathology and Medicine, Albert Einstein College of Medicine, Bronx, New York, USA^e

The aryl hydrocarbon receptor (AhR) is a ligand-activated transcription factor involved in controlling several aspects of immune responses, including the activation and differentiation of specific T cell subsets and antigen-presenting cells, thought to be relevant in the context of experimental *Trypanosoma cruzi* infection. The relevance of AhR for the outcome of *T. cruzi* infection is not known and was investigated here. We infected wild-type (WT) mice and AhR knockout (AhR KO) mice with *T. cruzi* (Y strain) and determined levels of parasitemia, myocardial inflammation and fibrosis, expression of AhR/cytokines/suppressor of cytokine signaling (SOCS) (spleen/heart), and production of nitric oxide (NO), reactive oxygen species (ROS), and peroxynitrite (ONOO⁻) (spleen). AhR expression was increased in the heart of infected WT mice. Infected AhR KO mice displayed significantly reduced parasitemia, inflammation, and fibrosis of the myocardium. This was associated with an anticipated increased immune response characterized by increased levels of inflammatory cytokines and reduced expression of SOCS2 and SOCS3 in the heart. *In vitro*, AhR deficiency caused impairment in parasite replication and decreased levels of ROS production. In conclusion, AhR influences the development of murine Chagas disease by modulating ROS production and regulating the expression of key physiological regulators of inflammation, SOCS1 to -3, associated with the production of cytokines during experimental *T. cruzi* infection.

The aryl hydrocarbon receptor (AhR) was originally described as a ligand-dependent transcription factor for exogenous ligands such as 2,3,7,8-tetrachlorodibenzo-*p*-dioxin (TCDD) capable of activating the aryl hydrocarbon hydroxylase (1, 2). In humans and mice, AhR recognizes several endogenous ligands, such as 6-formylindolo[3,2-*b*]carbazole (FICZ), kynurenines, indoles (3, 4), and lipoxins (LX) (5). The activation of the AhR signaling pathway controls the genomic expression of diverse target genes, leading to different physiological outcomes (6). More recently, it has been recognized that AhR is involved in the regulation of several immune processes. The major immune mechanisms controlled by AhR are related to the activation and differentiation of specific T cell subsets (T regulatory [Treg] and Th17) and antigen-presenting cells (3). In the context of immunity to infections, it was demonstrated that AhR is an essential protein for murine resistance to *Listeria monocytogenes* (7) and toxoplasmosis (8). More recently, we found that it was an important factor in controlling parasitemia and inflammation during experimental cerebral malaria (9). Additionally, it is associated with antiviral immunity (10) and is a negative regulator of inflammatory cytokines in response to *Leishmania major* experimental infection (11). Taken together, the results of these studies strongly suggest that AhR function during immune responses to infections is complex and likely pathogen specific.

Trypanosoma cruzi is a flagellated protozoan parasite that causes Chagas disease, an important neglected zoonosis affecting 6 to 7 million persons, with many millions at risk (12). Chagasic cardiomyopathy may develop in 20% to 40% of the infected persons (13). Interleukin-12 (IL-12)-dependent production of inter-

feron gamma (IFN- γ) is critical in controlling intracellular pathogen replication (14–17). Natural killer (NK) cells, when activated by IL-12, produce IFN- γ , resulting in an expansion of the populations of CD4⁺ and CD8⁺ T cells, which in turn produce further IFN- γ . IFN- γ activates *T. cruzi*-infected macrophages to produce nitric oxide (NO), which controls the intracellular replication of pathogens (18). The increased activity of reactive oxygen species (ROS) is a double-edged sword in the setting of *T. cruzi* infection. Although important in the inhibition of parasite replication, ROS may result in host cell damage. Interestingly, some reports suggest that ROS-derived metabolites may promote pathogen replication (19). Importantly, both NO and ROS are capable of promoting peroxynitrite-mediated *T. cruzi* clearance in macrophages (20, 21).

Suppressor of cytokine signaling (SOCS) genes compose a gene family controlled by AhR transcriptional activity (22). The SOCS

Received 8 July 2016 Accepted 27 July 2016

Accepted manuscript posted online 1 August 2016

Citation Barroso A, Gualdrón-López M, Esper L, Brant F, Araújo RRS, Carneiro MBH, Ávila TV, Souza DG, Vieira LQ, Rachid MA, Tanowitz HB, Teixeira MM, Machado FS. 2016. The aryl hydrocarbon receptor modulates production of cytokines and reactive oxygen species and development of myocarditis during *Trypanosoma cruzi* infection. *Infect Immun* 84:3071–3082. doi:10.1128/IAI.00575-16.

Editor: J. A. Appleton, Cornell University

Address correspondence to Fabiana S. Machado, machadofs@icb.ufmg.br.

A.B. and M.G.-L. contributed equally to this article.

Copyright © 2016, American Society for Microbiology. All Rights Reserved.

protein family is composed of eight proteins, commonly known as cytokine-inducible SH2-containing protein (CIS) and SOCS1 to -7. SOCS1 to -3 are the most intensively studied members and are associated with the suppression of cytokine signal transduction by inhibition of Janus kinase (JAK) activities. SOCS1 plays an important role as a negative regulator in IFN- γ signaling, while SOCS3 has a dual function, since it is able to inhibit simultaneously the signaling cascades triggered by proinflammatory and anti-inflammatory cytokines such as IL-6 and IL-10 (23). It is well known that the SOCS family members show cross-regulation, and SOCS2 might influence the activity of other family members such as SOCS1 and SOCS3 (23). Previously, we demonstrated that *Toxoplasma gondii* antigens stimulated AhR activation in dendritic cells and were associated with downstream expression of SOCS2 *in vitro* (5). Interestingly, we showed that SOCS2 was an important immune regulator in the pathogenesis of *T. cruzi*-induced cardiomyopathy in a murine model of Chagas disease (24). Indeed, in the absence of SOCS2, inflammatory and immune responses were reduced, resulting in infection-associated cardiac dysfunction (24).

It is known that AhR is important in controlling aspects of both innate and adaptive immune responses in several models of infection. In addition, SOCS2 (a gene target of AhR) is a relevant factor required for inflammatory/immune responses to *T. cruzi* infection. Therefore, we were interested in examining the role of AhR in the immune modulation and development of myocarditis during experimental *T. cruzi* infection by using an AhR knockout (AhR KO) mice model. Our findings indicate that AhR confers susceptibility to *T. cruzi* infection by mediating the negative regulation of ROS *in vivo* and the downregulation of proinflammatory cytokines necessary for adequate control of the parasite growth/dissemination.

MATERIALS AND METHODS

Ethics statement. This research study was carried out in strict accordance with the Brazilian Guidelines on animal work and the Guide for the Care and Use of Laboratory Animals of the National Institutes of Health (NIH). The animal ethics committee (CEUA) of the Universidade Federal de Minas Gerais (UFMG) approved all experiments and procedures, including euthanasia and fluid and organ removal (Permit Number 89/2010). All animal experiments were planned in order to minimize mouse suffering.

Animals. Wild-type (WT) C57BL/6 mice were obtained from the Animal Care Facilities of UFMG, Minas Gerais, Brazil. AhR knockout (KO) mice were bred on a C57BL/6 genetic background under pathogen-free conditions at the Instituto de Ciências Biológicas (ICB), UFMG.

Infection of mice and cells. The Y strain of *T. cruzi* was used for *in vivo* and *in vitro* experiments. WT and AhR KO mice were infected intraperitoneally (i.p.) with 1×10^3 trypomastigotes, and parasitemia levels were periodically measured in 5 μ l of blood from a tail vein (25). For *in vitro* infection, trypomastigotes were grown in cultures of a monkey kidney epithelial cell line (LLC-MK2) and then used for infection at a 5:1 parasite/host cell ratio.

Macrophage cultures, parasite uptake, microbicidal activity, and stimulation of *T. cruzi* antigens. Macrophages were harvested from peritoneal cavities as previously described (25) and plated (2×10^5 or 1×10^6 cell/well) onto culture plates (Nunc, Rochester, NY, USA). Infections were performed as described above. The number of intracellular amastigotes was determined in macrophages fixed and stained with *Panótico Rápido* (LB Laborclin, Pinhais, PR, Brazil) at 4 and 48 h postinfection to evaluate parasite uptake and intracellular growth, respectively. Parasite growth and survival were quantified by determining the number of re-

leased trypomastigotes in the supernatants from day 3 to day 7 day postinfection (dpi). *In vitro* stimulation of macrophages with *T. cruzi* antigens was performed by using 10 μ g/ml of a parasite lysate produced using a modification of a previously published protocol (26) for 6, 12, and 24 h and analyzed by immunoblotting.

Treatment with FeTPPS and quantification of peroxynitrite (ONOO⁻) and ROS production *in vitro*. Macrophages were obtained and cultivated as described above. After 2 h of *T. cruzi* infection, the macrophage cultures were incubated with 10 or 50 μ M 5,10,15,20-tetrakis(4-sulphonatophenyl) porphyrinato iron(III) (FeTPPS; Calbiochem, San Diego, CA, USA), a peroxynitrite scavenger. Parasite replication (48 h postinfection) and released trypomastigotes (3 to 7 dpi) were determined as described above. To estimate ONOO⁻ quantities, we incubated the cultures for 1 h at 37°C with 10 or 50 μ M FeTPPS followed by 25 μ M dihydrorhodamine 123 probe (DHR 123; Invitrogen, Carlsbad, CA) for 30 min at 37°C. Fluorescence was quantified by fluorimetry (Synergy 2; BioTek, Winooski, VT, USA). Data were expressed as fold change using arbitrary units of fluorescence. For ROS detection, we performed a real-time chemiluminescence assay as previously described (27). Macrophages were isolated and cultured (1×10^6 cells/well) overnight, followed by addition of 0.05 mM luminol (5-amino-2,3-dihydro-1,4-phthalazinedione) and zymosan A (both from Sigma-Aldrich Co.) (10:1 particle/cell ratio) and parasites to cell cultures. Light emission was quantified immediately after stimulation every 2 min during a 3-h period in a luminometer (Packard, Waltham, MA, USA). Data were represented as relative light units (RLU) and area under the curve (AUC).

Histopathology. At the indicated time points, mice were euthanized, hearts were removed and immediately fixed in 4% buffered formalin, and tissue fragments were embedded in paraffin. Tissue sections were stained with hematoxylin and eosin (H&E) and examined under light microscopy. Heart inflammation was scored by counting the total numbers of inflammatory cells in 30 microscope fields ($\times 40$) in serial tissue sections as previously described (28). Quantification of fibrosis was performed in a blind manner on 10 sections of the right and left ventricle free walls. The percentage of myocardial fibrosis was obtained from a graticule of 25 hits, at a final magnification of $\times 400$. Fibrosis coinciding with each hit was counted until a total of 250 hits were obtained for the heart of each mouse. The values were expressed as mean percentages of fibrosis at 10 and 15 dpi.

Tissue processing and immunoblot analysis. Spleen, hearts, and cultured macrophages were processed for protein extraction following standard procedures (29). Protein concentrations were determined by the Bradford method, and protein suspensions were used for immunoblot analysis as previously described (29). Quantification of the band intensity was performed using the ImageJ software freely available at <http://rsb.info.nih.gov/ij/>. Values were normalized by the use of β -actin or GAPDH (glyceraldehyde-3-phosphate dehydrogenase). Mouse anti-AhR (Abcam, Cambridge, United Kingdom), β -actin (Sigma, St. Louis, MO, USA), and GAPDH (Cell Signaling, Danvers, MA, USA) antibodies were used.

Quantification of NO in serum. NO was quantified at 10 and 15 dpi as nitrite (NO₂⁻) by the Griess method (30). Nitrites (NO₃⁻) were reduced to nitrites by enzymatic conversion by nitrate reductase (31) (Roche, South San Francisco, CA, USA). The resulting NO₂⁻ concentration was determined by reference to a sodium nitrite standard curve.

Measurement of NO, ROS, and ONOO⁻ quantities *ex vivo*. Isolated splenic cells were obtained from mice at 10 dpi and cultured (1×10^6 cells/well) and incubated for 30 min at 37°C with 10 μ M 4,5-diaminofluorescein diacetate solution probe (DAF-2DA; Sigma) to estimate levels of detected intracellular NO or with 50 μ M 2',7'-dichlorodihydrofluorescein diacetate probe (H₂DCFDA; Invitrogen) to estimate levels of detected ROS or for 1 h with 10 μ M FeTPPS followed by 30 min with 25 μ M DHR 123 probe to estimate levels of detected ONOO⁻, as described in reference 32. For all analyses, samples were quantified by fluorimetry. Data were expressed as fold change in arbitrary units of fluorescence.

Flow cytometry. Splenic cells from infected and control mice were evaluated *ex vivo* for the expression of extracellular molecules, intracellu-

TABLE 1 Primer sets used for PCR analyses

Analyte	Forward primer	Reverse primer
18S	CTCAACACGGGAAACCTCA	CGTTCCACCAACTAAGAACG
AhR	CGGAGCGCTGCTTCCCTCCAC	GCTGCCCTTTGGCATCACAACC
Foxp3	CCCAGGAAAGACAGCAACCTT	TTCTCACAACCAGGCCACTTG
GAPDH	ACG GCCGCATCTTCTTG TGA	CGGCCAAATCCGTTACACCCGA
IFN- γ	TGAACGCTACACACTGCATCTTGG	CGACTCCTTTTCCGCTTCTGAG
IL-6	TTCCATCCAGTTGCCTTCTTG	TTGGGAGTGGTATCCTCTGTGA
IL-10	GCTCTTACTGACTGGCATGAG	CGCAGCTCTAGGAGCATGTG
IL-12p40	GCTGGACCCTTGCATCTGGCG	GGTGGCCAAAAAGAGGAGGTAGCG
IL-17A	TCCAGAAGGCCCTCAGACTA	TGAGCTTCCCAGATCACAGA
SOCS1	GCATCCCTCTTAACCCGGTAC	AATAAGGCGCCCCACTTA
SOCS2	CGCGTCTGGCGAAAGC	TTCTGGAGCCTCTTTTAATTTCTCTT
SOCS3	TTTGCGCTTTGATTTGGTTTTG	TGGTATTTTCTTTGGCCAGCA
TNF	ACGGCATGGATCTCAAAGAC	AGATAGCAAATCGGCTGACG
<i>T. cruzi</i> 18S	TTGTTTGGTTGATTCGGTCA	CCCAGAACATTGAGGAGCAT

lar cytokines, and ROS at 10 dpi. Cell suspensions were prepared as previously described (9). Each sample comprised individual mice splenic cell suspensions that were stained with specific combinations of antibodies: CD8 (peridinin chlorophyll protein [PerCP]), CD4 (Pacific Blue), IFN- γ (Alexa Fluor 488), CD11c (phycoerythrin [PE]-Cy7), IL-12 p70 (PE), F4/80 (allophycocyanin [APC]-Cy7), inducible nitric oxide synthase (iNOS) (fluorescein isothiocyanate [FITC]), ROS (H₂DCFDA), and isotype controls (all from BD Pharmingen, San Jose, CA, USA). Data were acquired on a FACScan system (BD, San Jose, CA, USA), and viable cells were analyzed by flow cytometry using FlowJo software (Tree Star, Ashland, OR, USA).

Total RNA extraction, cDNA production, and PCR. Splenic and cardiac tissues (30 mg) were removed 10 and 15 dpi, and total RNA was isolated. mRNA levels of IL-12 and IFN- γ were analyzed by reverse transcription-PCR (RT-PCR) and normalized by β -actin. Real-time quantitative PCR (qPCR) was performed on an ABI Prism StepOne sequence detection system (Applied Biosystems, Carlsbad, CA, USA) using SYBR green PCR master mix (Applied Biosystems) for the genes encoding IL-6, tumor necrosis factor (TNF), IL-17A, Foxp3, IL-10, SOCS1, SOCS2, and SOCS3. GAPDH or 18S genes were used as an endogenous control for normalization. The relative expression levels of genes were determined by the $2^{-\Delta\Delta CT}$ threshold cycle method and represented as fold change. The sequences of primers used in this study are shown in Table 1.

Parasite load quantification in heart. Heart tissue was removed 10 and 15 dpi and processed as described above. qPCR was performed with primers for *T. cruzi* 18S (the sequence is described above). Data were analyzed by taking a *T. cruzi* curve as a parameter for absolute quantification and were expressed as fold change.

Quantification of cytokines in supernatants of *ex vivo* cell cultures. Spleens were removed from *T. cruzi*-infected WT and AhR KO mice after 10 dpi and splenocytes plated (1×10^6 cells/well) followed by 48 h of incubation. Supernatants of cells were collected and used to quantify IL-12p40 and IFN- γ by enzyme-linked immunosorbent assay (ELISA) as previously described (24).

Statistical analysis. First, we performed a Shapiro-Wilk normality test for each data table to verify whether the data came from a Gaussian distribution. Next, when data were normally distributed, differences were compared by using Student's *t* test or analysis of variance (ANOVA) or two-way ANOVA followed by Bonferroni corrections as needed for multiple comparisons (Graph Prism software 4.0). Results are shown as means \pm standard errors of the mean (SEM). Results with a *P* value of <0.05 were considered significant.

RESULTS

AhR is upregulated in the heart but not in the spleen during *T. cruzi* infection. To investigate the involvement of AhR during *T.*

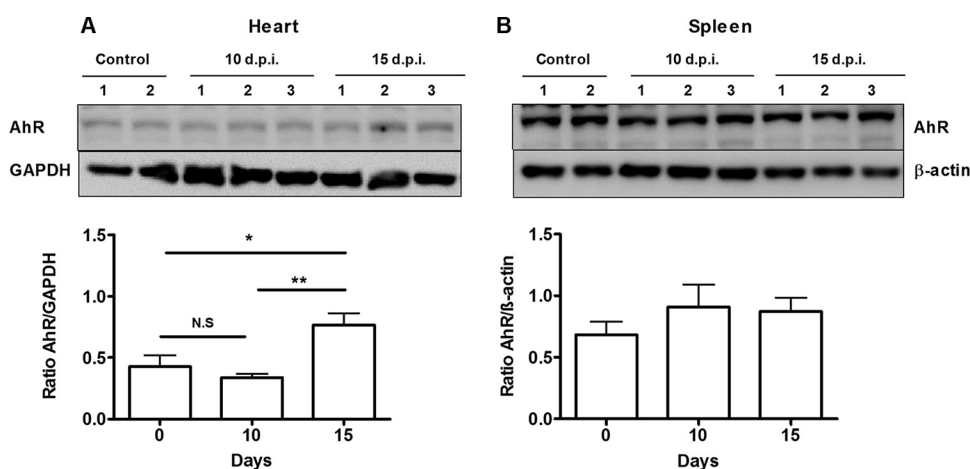


FIG 1 *T. cruzi* infection modulates AhR expression. WT mice were infected with 1×10^3 trypomastigotes of the Y strain. Hearts (A) and spleens (B) were harvested, and AhR protein levels were measured by Western blotting at 0 (control; 2 mice), 10 (10 d.p.i.; 3 mice), and 15 (15 dpi; 3 mice) days postinfection. For analysis, data were normalized to GAPDH and β -actin expression. Each point represents the mean \pm standard error of the mean (SEM) of data from three independent experiments. **, *P* < 0.01 ; *, *P* < 0.05 ; N.S., not significant.

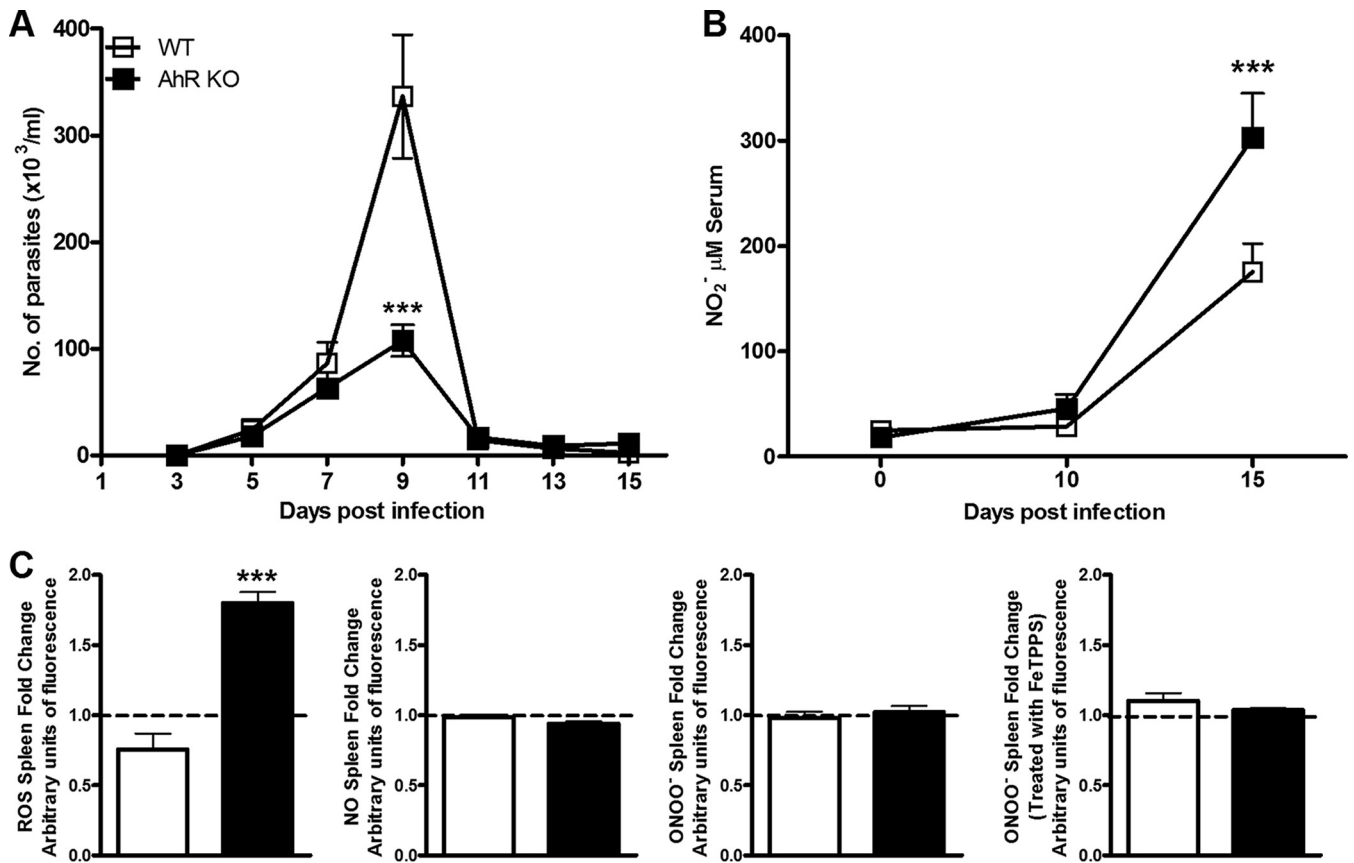


FIG 2 Regulation of ROS production during *T. cruzi* infection. WT and AhR KO mice were infected with 1×10^3 trypomastigotes. (A) Parasitemia was measured every 2 days from day 3 to day 15 postinfection (dpi). (B) Nitric oxide (NO) levels were measured in the serum of *T. cruzi*-infected AhR KO and WT mice by the Griess method following enzymatic conversion of NO_3^- to NO_2^- by nitrate reductase at 10 and 15 dpi. (C) Splens from *T. cruzi*-infected AhR KO and WT mice were obtained 10 dpi for *ex vivo* measurement of levels of reactive oxygen species (ROS) and of production of NO and also peroxynitrite (ONOO^-) after treatment with FeTPPS ($50 \mu\text{M}$) for 1 h or in the absence of treatment. Data are shown as means \pm SEM of the number of the parasites per milliliter of blood from one experiment representative of three independent experiments performed with seven animals per group for the data shown in panel A. Data were normalized to the results from AhR KO and WT noninfected animals and are represented as fold changes in panel C. ***, $P < 0.001$; *, $P < 0.05$.

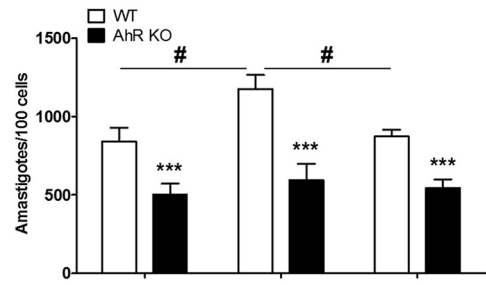
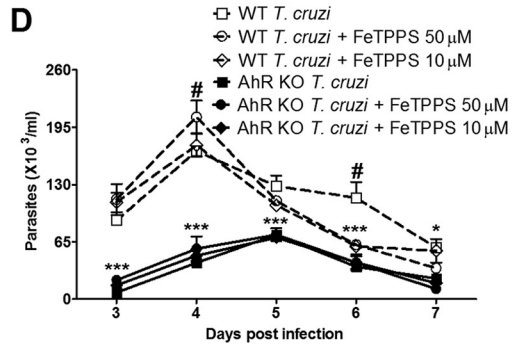
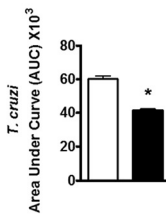
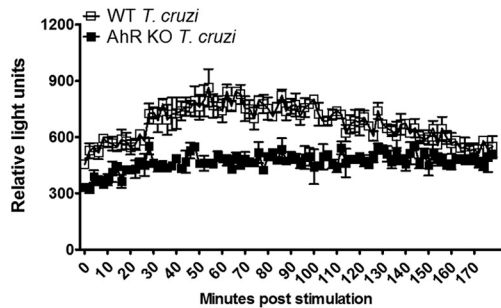
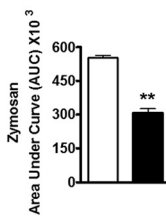
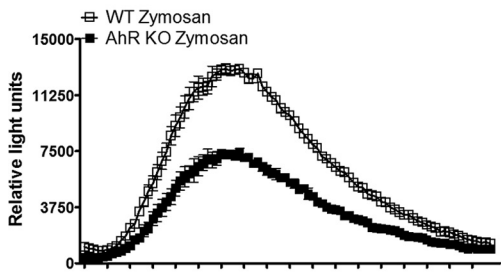
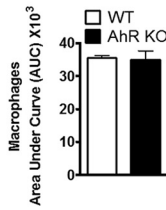
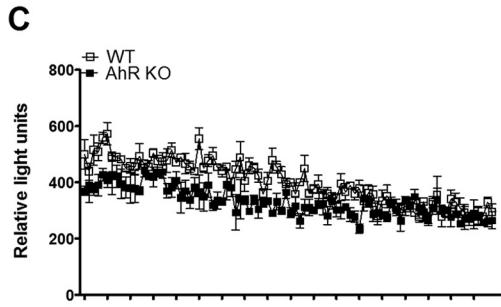
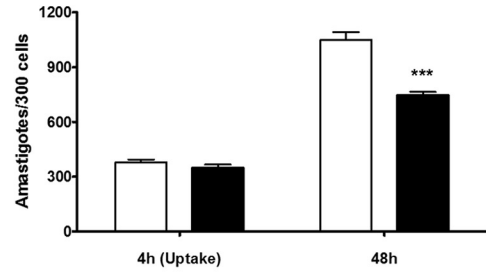
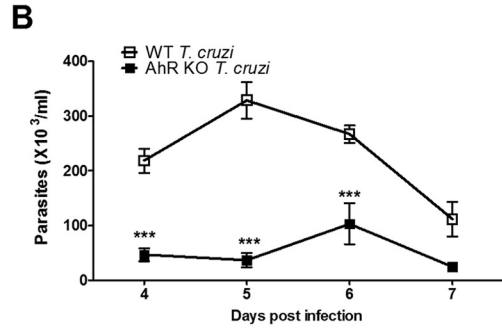
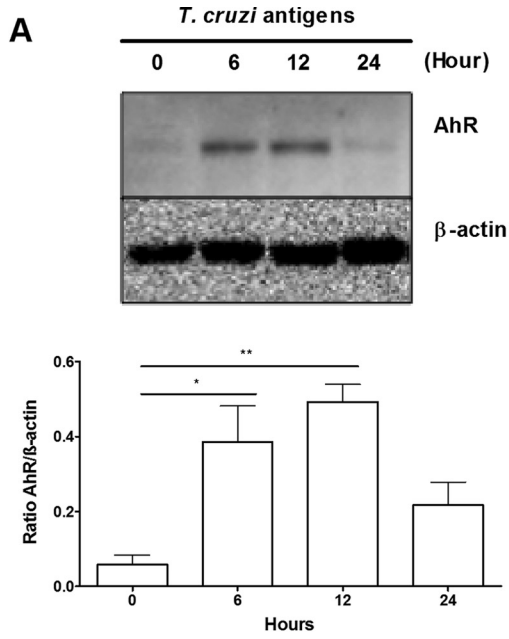
cruzi infection, we determined AhR protein expression levels in relevant organs of infected WT mice by Western blotting. We found that AhR was upregulated in the heart (Fig. 1A) of infected WT mice at 15 days postinfection (dpi). In contrast, AhR protein levels in the spleen were not affected by *T. cruzi* infection (Fig. 1B).

Deficiency of AhR results in a reduction of parasitemia. To understand AhR function, we first studied the control of parasite replication during the acute phase of infection. We infected WT and AhR KO mice and determined parasitemia until 15 dpi. We found that AhR KO mice displayed a significant reduction in parasitemia at 9 dpi compared with the WT counterparts (Fig. 2A). This result demonstrates that AhR plays a role in parasite replication during *T. cruzi* infection.

Increased levels of ROS, but not of NO and ONOO^- , are produced in the spleen of *T. cruzi*-infected AhR KO mice. As ROS, ONOO^- , and NO are important cytotoxic mediators during *T. cruzi* infection and AhR has been found to be involved in the control of ROS metabolism activity against intracellular pathogens (33), we analyzed the levels of these molecules in *T. cruzi*-infected WT and AhR KO mice. First, we measured systemic nitrite levels in the serum of infected WT and AhR KO mice and found that nitrite concentrations were significantly increased 15

dpi in AhR KO mice compared with WT mice (Fig. 2B). Notably, this amount of nitrite in AhR KO mice was at a time point after parasitemia was controlled (Fig. 2A). Next, we analyzed the *ex vivo* production of these molecules by splenocytes of infected mice. We found that AhR deficiency resulted in increased production of ROS but not of NO and ONOO^- compared with WT mice at 10 dpi (Fig. 2C). In fact, addition of FeTPPS, a drug that functions as an ONOO^- scavenger, did not change the levels of ONOO^- detected by the DHR 123 probe, suggesting that expression of ONOO^- was not induced in splenocytes during the infection (Fig. 2C).

Deficiency of AhR results in a reduction of *in vitro* ROS production and decreases the *T. cruzi* burden in macrophages. Macrophages are important cells targeted by *T. cruzi* in our experimental model. These cells are equipped with cytotoxic mechanisms responsible for parasite death (34, 35). Therefore, we wanted to explore if the absence of AhR in these cells contributed to the reduced parasitemia observed *in vivo* in the *T. cruzi*-infected AhR KO mice. We purified WT macrophages and stimulated them *in vitro* with a suspension of *T. cruzi* antigens (TcAg) in order to determine if these cells respond to *T. cruzi* by upregulating AhR. Our results clearly demonstrated that AhR expression increased significantly after 6 and 12 h of *in vitro* stimulation with



<i>T. cruzi</i>	+	+	+
FeTPPS 50 μ M	-	+	-
FeTPPS 10 μ M	-	-	+

10 $\mu\text{g/ml}$ of TcAg, followed by a decrease of expression after 24 h (Fig. 3A). When cultured macrophages obtained from AhR KO mice were infected, increased microbicidal activity was observed. The numbers of released trypomastigotes and intracellular amastigotes were significantly reduced in these cells compared with WT cells (Fig. 3B). This was not associated with a defect in parasite entry, since uptake assays (4 h) displayed no difference between WT and AhR KO cells in the numbers of amastigotes (Fig. 3B). Next, we investigated the ability of AhR-deficient macrophages to produce NO and ROS since the members of this group of molecules are major cytotoxic mediators involved in clearance of intracellular pathogens by macrophages (33, 34, 36). We did not observe any differences in the amounts of NO released by *T. cruzi*-infected macrophages from the two groups of mice (data not shown). Furthermore, we quantified the real-time production of ROS molecules and found that noninfected AhR-deficient macrophages produced basal levels of ROS similar to those seen with WT cells (Fig. 3C). However, the deficiency of AhR resulted in a significant decrease in the production of ROS by macrophages stimulated with zymosan or infected by *T. cruzi* (Fig. 3C), indicating that *in vitro* ROS production by macrophages is partially dependent on the presence of AhR. In order to fully demonstrate that ONOO⁻ is not the main molecule involved in the clearance of parasites in the AhR KO mice, we infected macrophages following *in vitro* incubation with FeTPPS. The amounts of released trypomastigotes and the intracellular amastigotes remained lower in AhR KO cells than in WT cells (Fig. 3D). However, consumption of ONOO⁻ in WT-infected cells resulted in increased release of trypomastigotes (until 7 dpi) and intracellular amastigote replication (at 48 h) (Fig. 3D). Collectively, these results strongly suggest that AhR mediates, in part, the *in vitro* production of ROS by *T. cruzi*-infected macrophages.

Deficiency of AhR is associated with a robust proinflammatory response in the spleen of *T. cruzi*-infected mice. IL-12 and IFN- γ are important cytokines released during innate and acquired immune responses to control *T. cruzi* infection (13). Several reports have suggested that AhR is part of a regulatory pathway that inhibits the proinflammatory response in several models of infection (8, 9, 11). In order to ascertain whether this was the case in *T. cruzi* infection, we used flow cytometry to evaluate the production of these cytokines by different immune cell populations in the spleen at 10 dpi. We found a significant increase in the numbers of dendritic cells (CD11c⁺ CD8⁺ IL-12⁺) and macrophages (CD11b⁺ F4/80⁺ IL-12⁺) (Fig. 4A) and of T cells (CD3⁺ CD8⁺ IFN- γ ⁺ and CD3⁺ CD4⁺ IFN- γ ⁺) (Fig. 4B) in the spleen of *T. cruzi*-infected AhR KO mice compared to their WT counterparts. The increased amounts of IL-12p40 and IFN- γ were also evident when we used ELISA to analyze the *ex vivo* production of these cytokines by total splenocytes (Fig. 4A and B, respectively).

Consistent with the increased amount of ROS observed by chemiluminescence in AhR KO splenocytes (Fig. 2C), we also observed that the number of splenic macrophages producing ROS (CD11b⁺ F4/80⁺ ROS⁺) in AhR KO mice was significantly higher than in infected WT mice (Fig. 4C). No other cell population (i.e., granulocytes or lymphocytes) showed prominent ROS production upon *T. cruzi* infection (data not shown), suggesting that macrophages are the predominant cell type producing ROS in the spleen as a result of *T. cruzi* infection. Importantly, we also found that at this time point of infection, the number of CD11b⁺ F4/80⁺ iNOS⁺ macrophages was also augmented in the spleen of AhR KO mice, indicating that NO may be actively produced (Fig. 4C). To further characterize the profile of the acquired immune response, we also analyzed the proportions of the different T helper and regulatory cell populations present in the spleen of WT and AhR KO mice. We found that the absence of AhR resulted in an increase in the number of Th1 (CD3⁺ CD4⁺ IFN- γ ⁺) and Th2 (CD3⁺ CD4⁺ IL-10⁺) cells in response to *T. cruzi* infection, but not in the number of Th17 (CD3⁺ CD4⁺ IL-17⁺) or Treg (CD3⁺ CD4⁺ CD25^{hi} Foxp3⁺) cells, compared to the levels seen with WT mice (Fig. 4D). In a complementary study, we also evaluated mRNA levels of other cytokines and molecules important for immune regulation such as IL-6, TNF, IL-17, and IL-10, the transcription factor Foxp3, and SOCS1, SOCS2, and SOCS3 at 10 and 15 dpi. We found that levels of proinflammatory cytokines (IL-6, TNF, and IL-17) were increased as a result of infection in both WT and AhR KO mice. No differences in IL-6 and TNF mRNA levels (Fig. 5A) were observed in comparisons of infected AhR KO and WT mice. In contrast, levels of IL-17 (Fig. 5A) were significantly higher in AhR KO mice than in WT mice at 10 dpi. The mRNA levels of Foxp3, the marker transcription factor of Treg cells, were significantly upregulated at 15 dpi (Fig. 5A), while the levels of the regulatory IL-10 cytokine (Fig. 5B) were reduced in AhR KO mice at the same time point compared with the WT counterparts. Our analyses also revealed that mRNA expression of SOCS1, SOCS2, and SOCS3 was increased in infected AhR KO mice compared with WT mice (Fig. 5B).

***T. cruzi*-induced heart inflammation is reduced in the absence of AhR.** The heart is an important target organ of *T. cruzi* infection. The histology of hearts obtained from WT and AhR KO mice was normal (Fig. 6A, D, G, and J). We observed that *T. cruzi* infection induced a poor inflammatory response (Fig. 6B, E, and M) and less fibrosis (Fig. 6H, K, and N) in WT and AhR KO mice at 10 dpi. The quantity of inflammatory cells increased by 15 dpi and was significantly lower in the hearts of AhR KO mice (Fig. 6C, F, and M). As a consequence, fibrosis was reduced in hearts of *T. cruzi*-infected AhR KO mice compared with the WT counterparts (Fig. 6I, L, and N). The absolute quantification of parasite burden in the heart showed a significant increase at 10 dpi in AhR KO

FIG 3 AhR modulates ROS production and *T. cruzi* replication in macrophages. (A) WT peritoneal macrophages were cultured, and after 6, 12, and 24 h of *in vitro* stimulation with 10 $\mu\text{g/ml}$ of *T. cruzi* antigen (TcAg), AhR expression was analyzed by Western blotting. (B) WT and AhR KO peritoneal macrophages were cultured and infected with *T. cruzi* (5:1 parasite/cell ratio), and the amounts of trypomastigotes in supernatants of *T. cruzi*-infected WT and AhR KO macrophages from 4 to 7 dpi were quantified. Intracellular amastigotes were counted in 300 macrophages at 4 h (Uptake) and 48 h (growth) postinfection. (C) Reactive oxygen species (ROS) production was measured by real-time chemiluminescence analysis in WT and AhR-deficient macrophages cultured with medium alone, zymosan (10:1 particle/cell ratio), or trypomastigotes (5:1 parasite/cell ratio), and data were quantified as relative light unit (RLU) and area under the curve (AUC) values. (D) The numbers of trypomastigotes in supernatants of WT and AhR KO *T. cruzi*-infected macrophages treated or not treated with FeTPPS (10 or 50 μM) after 2 h of infection from 3 to 7 dpi were counted. Each point represents means \pm SEM of the results of three independent experiments in triplicate samples. In panel D, asterisks (*) indicate analyses consisting of comparisons between WT Tc and AhR KO Tc, and pound signs (#) indicate analyses consisting of comparisons between WT Tc and WT Tc plus FeTPPS. ***, $P < 0.001$; **, $P < 0.01$; *, $P < 0.05$.

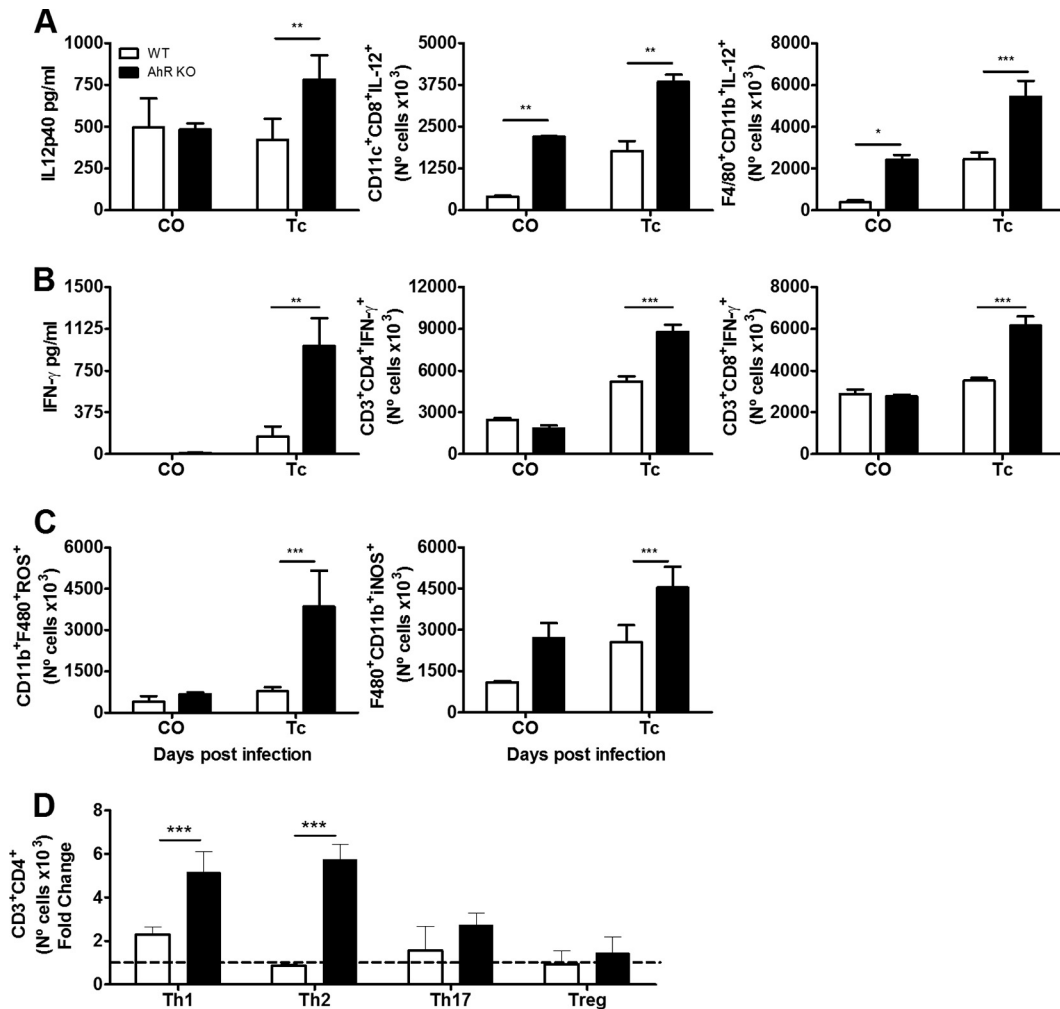


FIG 4 Increased proinflammatory responses are induced in the spleen of *T. cruzi*-infected AhR KO mice. WT and AhR KO mice were infected with 1×10^3 trypomastigotes. Spleens of *T. cruzi*-infected WT and AhR KO mice were processed and analyzed by ELISA and flow cytometry 10 days postinfection (dpi). (A to C) *Ex vivo* measurements by ELISA of IL-12p40 and IFN- γ levels were performed in supernatants of splenocytes cultured for 48 h (A and B, respectively). After extracellular and intracellular staining, cell numbers of the following cell populations were quantified by flow cytometry: CD11c⁺ CD8⁺ IL-12 p70⁺ and F4/80⁺ CD11b⁺ IL-12 p70⁺ (A); CD3⁺ CD4⁺ IFN- γ ⁺ and CD3⁺ CD8⁺ IFN- γ ⁺ (B); and CD11b⁺ F4/80⁺ ROS⁺ and CD11b⁺ F4/80⁺ iNOS⁺ (C). (D) Proportions of different T helper and regulatory cell populations Th1 (CD3⁺ CD4⁺ IFN- γ ⁺), Th2 (CD3⁺ CD4⁺ IL-10⁺), Th17 (CD3⁺ CD4⁺ IL-17⁺), and Treg (CD3⁺ CD4⁺ CD25^{hi} Foxp3⁺). The results represent control uninfected (CO) mice and mice infected with *T. cruzi* (Tc) (A to C) or were normalized to the results determined for AhR KO and WT noninfected animals and represent fold change in panel D. Analyses were performed as comparisons between *T. cruzi*-infected WT mice and infected AhR KO mice. Data are presented as means \pm SEM and represent results of three independent experiments performed with four animals each. ***, $P < 0.001$; **, $P < 0.01$; *, $P < 0.05$.

mice compared with the WT mice; however, this increase was not statistically significant at 15 dpi (Fig. 6O). To further characterize the inflammatory profile observed in the heart, we determined the mRNA levels of proinflammatory cytokines IL-12, IFN- γ , IL-6, TNF, IL-17; the anti-inflammatory cytokine IL-10; and the cytokine signal regulators SOCS1, SOCS2, and SOCS3. We found that both groups displayed a significant increase in the mRNA levels of proinflammatory cytokines (IL-12, IL-6, TNF, IFN- γ , and IL-17) (Fig. 7A), reflecting intense infection-induced inflammation. The mRNA levels of the majority of these molecules were significantly augmented in the absence of AhR, with the remarkable exception of IFN- γ (Fig. 7A), the level of which was, in contrast, significantly reduced compared to that seen with WT mice. The levels of the Treg cell molecular marker Foxp3 and the regulatory cytokine IL-10 (Fig. 7B) were initially augmented upon infection and

were then reduced by 15 dpi; this was observed in both groups of mice (Fig. 7B). We also examined the expression of SOCS1, SOCS2, and SOCS3 genes in the hearts of infected WT and AhR KO mice. Expression of these molecules was significantly increased at 10 dpi in WT mice (Fig. 7B). However, and in contrast to what we found in the spleen, we observed a significant reduction in mRNA levels of SOCS2 and SOCS3, but not of SOCS1, in the absence of AhR (Fig. 7B).

DISCUSSION

AhR is an important factor in the immune system, especially as it relates to autoimmunity and infection (3, 37). Here, we found a previously unrecognized role of AhR in the regulation of the immune response during *T. cruzi* infection. The following major findings were obtained in the present study: (i) AhR is upregulated in

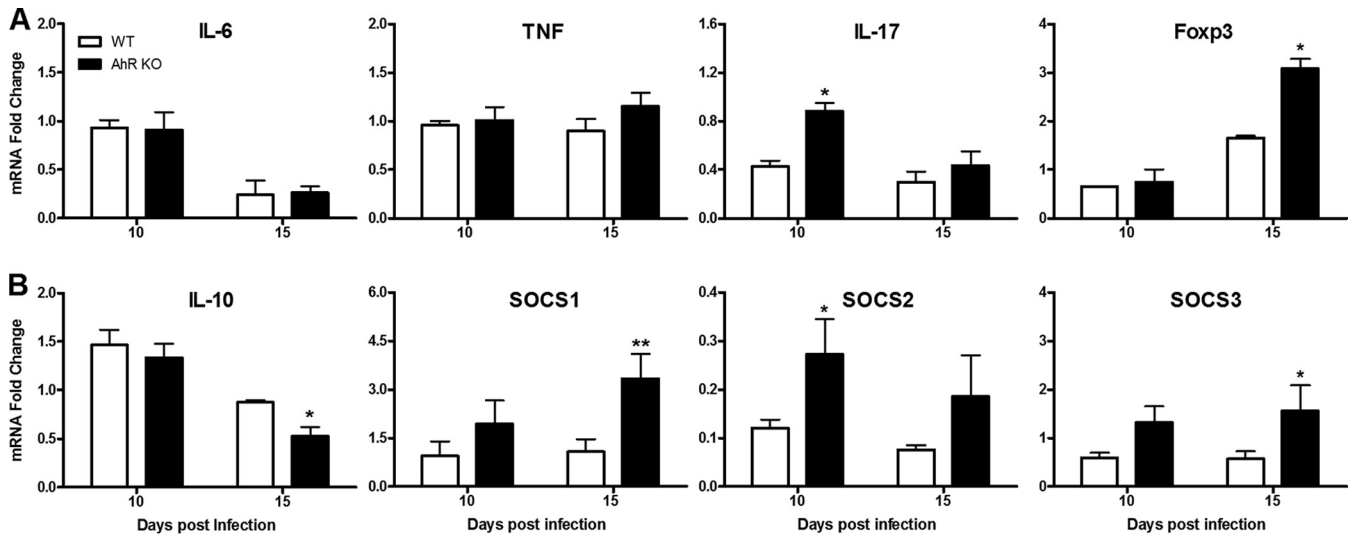


FIG 5 Cytokine and SOCS profiles in the spleen of *T. cruzi*-infected AhR KO and WT mice. WT and AhR KO mice were infected with 1×10^3 trypomastigotes. Splens of *T. cruzi*-infected WT and AhR KO mice were processed for total RNA extraction. mRNA levels of IL-6, TNF, IL-17A, and Foxp3 (A) and of IL-10, SOCS1, SOCS2, and SOCS3 (B) were quantified 10 and 15 days postinfection (dpi) by quantitative RT-PCR (qRT-PCR) and are represented as $2^{-\Delta\Delta CT}$ values. Data were normalized to those of uninfected WT or AhR KO mice. Data are presented as means \pm SEM and represent the results of two independent experiments. **, $P < 0.01$; *, $P < 0.05$.

the heart of *T. cruzi*-infected WT mice, as well as in macrophages infected *in vitro*; (ii) absence of AhR results in a reduction of parasitemia and pathology (i.e., inflammation and fibrosis) in the heart, although it also decreases expression of SOCS2, an important protein preventing myocardial dysfunction during *T. cruzi* infection, in the heart; (iii) AhR deficiency results in an increased oxidative burst in splenic macrophages and in a potent proinflammatory cytokine response; and (iv) the absence of AhR in macrophages, in contrast, leads to impaired replication of *T. cruzi in vitro*, despite a decrease in ROS production and no change in NO production.

AhR is expressed in immune cells in many organs (4). Our studies demonstrated that *T. cruzi* infection causes an increase in AhR expression in the heart, but not in the spleen, at 15 dpi. AhR is expressed and activated in cardiac cells during mouse heart embryogenesis and in adulthood (38). Increased expression of AhR in response to *T. cruzi* infection in this tissue could be explained by the presence of inflammatory infiltrate and/or by specific AhR expression in infected cardiac myocytes.

In macrophages stimulated *in vitro* with *T. cruzi* antigens, the upregulation of AhR indicates that *T. cruzi*-derived-pathogen-associated molecular patterns (PAMPs) are responsible for the activation of specific signaling pathways that induce AhR transcription and translation in these cells. Recent studies demonstrated that ROS initiates signaling cascades through the transcription nuclear factor kappa B (NF- κ B), leading to AhR transcription and activation (39, 40). Other reports have indicated that *T. cruzi* activates the NF- κ B signaling pathway (41). Taken together, these observations allow us to hypothesize that the activation of NF- κ B during *T. cruzi* infection results in AhR transcription and activation.

The significant reduction in parasitemia in the AhR KO mice reveals a crucial role for this receptor in *T. cruzi* infection. Similarly, macrophages from AhR KO mice controlled parasite replication more effectively than WT cells. Parasitemia control is achieved via several immune mechanisms (18–21). However, our

results strongly suggest that the resistant phenotype observed in AhR KO mice could be explained by factors such as production of larger amounts of systemic NO, an important molecule involved in parasite clearance (42). Our results demonstrated a significant increase in the number of inflammatory macrophages (CD11b⁺ F4/80⁺ iNOS⁺) at 10 dpi in the spleen of infected AhR KO mice compared to WT mice, suggesting that this population could be responsible for the systemic accumulation of NO observed at 15 dpi, thus contributing to the reduced parasitemia. Our *ex vivo* results also demonstrated that at 10 dpi, splenocytes obtained from AhR KO mice produced increased levels of ROS compared to those from the WT mice. However, this was not accompanied by an increase in ONOO⁻ production, likely due to the fact that at 10 dpi, we did not detect an increase in NO production under the same conditions. ONOO⁻ production is dependent on the presence of NO and O₂⁻ at approximately equimolar concentrations in the same compartment (43). Therefore, an increase in superoxide alone could not drive an increase in ONOO⁻ production. Supporting these data indicating more ROS production in spleen cell cultures, we found that the number of macrophages producing ROS (CD11b⁺ F4/80⁺ ROS⁺) was also increased in splens from infected AhR KO mice. This indicates that AhR is an important negative regulator of oxidative bursts during *in vivo T. cruzi* infection.

It is well established that ROS act as rapid mediators of innate immune cells to eliminate intracellular pathogens and that this is coupled to antioxidant mechanisms to prevent cell damage (35). Several reports have linked AhR to the response mediated by nuclear factor erythroid 2-related factor (Nrf2) in various cell types where the two transcription factors act synergistically in the xenobiotic and antioxidant response (4). The increased production of ROS *in vivo*, as seen in AhR KO mice, could be explained by the inability of macrophages to activate an antioxidant response in the absence of AhR while responding to *T. cruzi* infection. Thus, high cytotoxicity mediated by NO and ROS in macrophages could

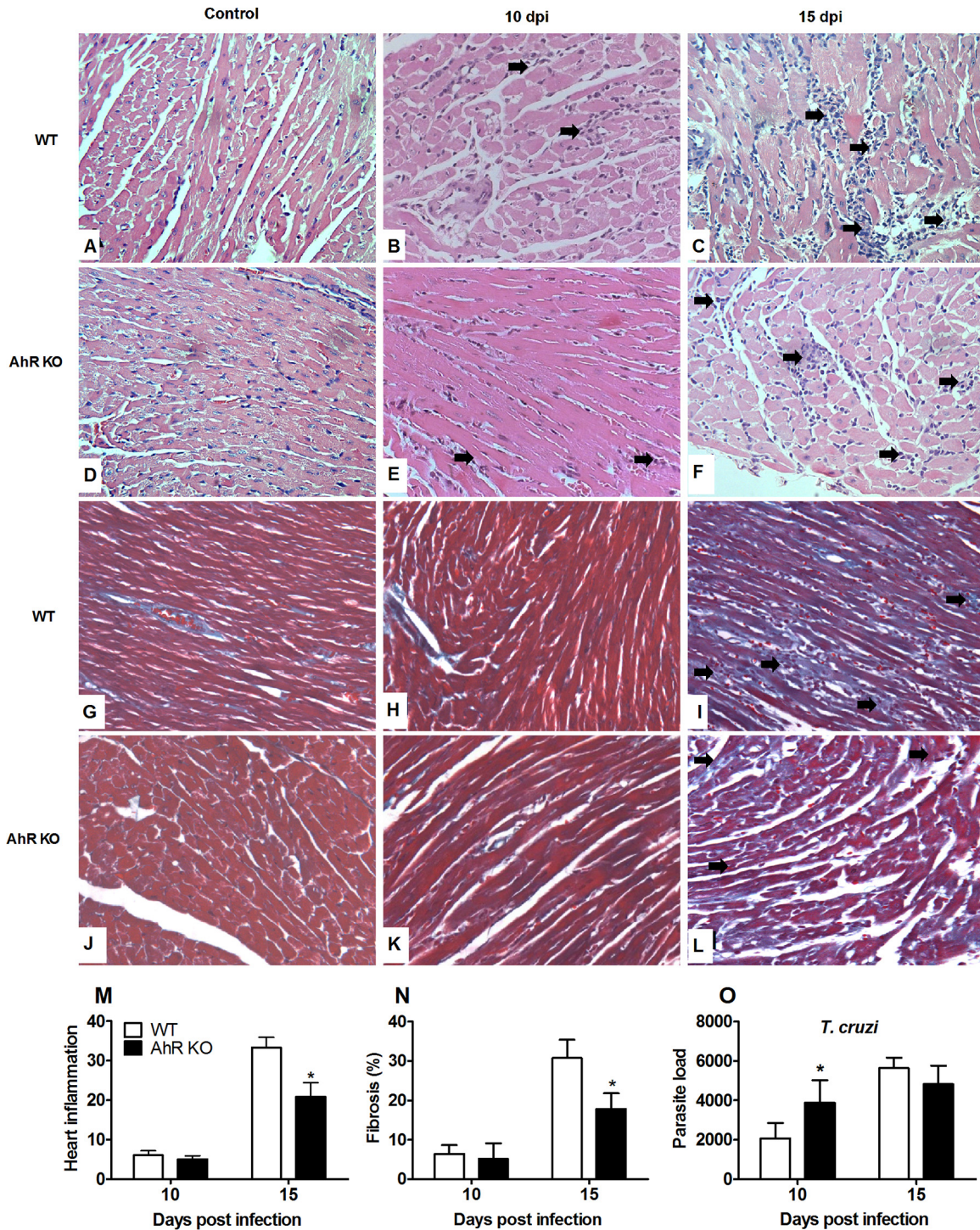


FIG 6 Absence of AhR results in decreased inflammatory cells in heart of *T. cruzi*-infected mice. WT and AhR KO mice were infected with 1×10^3 trypomastigotes. Hearts of *T. cruzi*-infected WT and AhR KO mice were harvested and processed and stained with H&E, and sections were cut from uninfected and *T. cruzi*-infected WT and AhR-deficient mice to quantify the inflammatory infiltrate and fibrosis. Panels A and D depict the normal histological appearance in uninfected animals. Panels B and E depict discrete and multifocal infiltration of immune cells in myocardium from both infected groups (arrows) at 10 days postinfection (dpi). Panel C depicts multifocal to coalescing and intense inflammatory infiltration in the myocardium (arrows) at 15 dpi. Panel F depicts multifocal and moderate myocarditis (arrows). Panels G and J depict normal myocardium from an uninfected mouse. Panels H and K depict minimal deposition of collagen from both infected groups at 10 dpi. (I and L) Intense myocardial fibrosis of an infected WT mouse (I, arrows) and mild fibrosis in AhR KO infected mouse 15 dpi (L, arrows). Original magnification in panels A to F, $\times 400$. Heart inflammation (M), fibrosis (N), and parasite load (O) were scored at 10 and 15 dpi. Data are shown as means \pm SEM. *, $P < 0.05$.

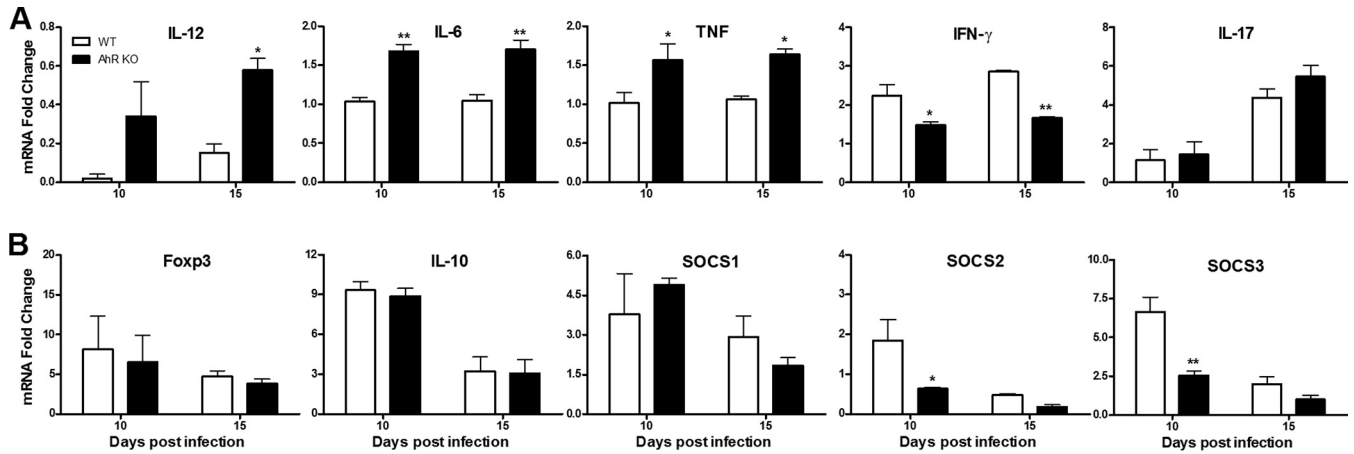


FIG 7 Cytokine profile in the heart of *T. cruzi*-infected AhR KO and WT mice. WT and AhR KO mice were infected with 1×10^3 trypomastigotes. Total RNA was extracted from the hearts of *T. cruzi*-infected WT and AhR KO mice. mRNA levels of IL-12, IL-6, TNF, IFN- γ , and IL-17A (A) and of Foxp3, IL-10, SOCS1, SOCS2, and SOCS3 (B) were measured 10 and 15 days postinfection (dpi). mRNA levels of IL-12 and IFN- γ were measured by RT-PCR, while the levels of the remaining cytokines were measured by qPCR. Data were normalized to those determined for uninfected WT or AhR KO mice and are represented as $2^{-\Delta\Delta CT}$ values. Data are presented as means \pm SEM and are from one experiment representative of two independent experiments. **, $P < 0.01$; *, $P < 0.05$.

result in improved control of parasite replication in the absence of AhR.

Interestingly, our studies revealed a different involvement of AhR in ROS production during *in vitro* *T. cruzi* infection. The absence of AhR resulted in the reduction of ROS production in infected macrophages even though parasite replication levels were lower in AhR KO macrophages. We consistently found decreased ROS production by AhR KO macrophages in the presence of zymosan, a stimulus that typically induces ROS in the setting of phagocytosis (44). Previously, it was reported that AhR contributes substantially to ROS production when cells are persistently activated by TCDD and that this is mediated by persistent CYP1 expression (19, 45, 46). The contradiction between ROS production by spleen cells from infected mice *ex vivo* and by macrophages stimulated *in vitro* could be explained by the wide range of ligands that can differentially activate AhR and the vast quantity of genes that are under AhR control (6). Therefore, *in vivo* responses, where cells are in complex environments, are contrasted to the *in vitro* response, such as in our *in vitro* system, where infected macrophages lack other stimuli such as the interactions with other cells, cytokines, and immune complexes.

Recently, it was demonstrated that ROS, besides its potent prooxidant effect on intracellular pathogens, can also be beneficial for *T. cruzi* replication *in vitro* (35, 47). It has been shown that *T. cruzi* can sequester iron from ferritin upon oxidative burst (19), providing an explanation for the defect in parasite replication observed in AhR KO macrophages. In addition, scavenging of ONOO $^-$ did not alter the parasite growth observed in AhR KO macrophages, suggesting that the reduced parasite growth in AhR-deficient macrophages is not associated with ONOO $^-$. Our *in vitro* experiments demonstrated that deficiency of AhR did not change NO levels but resulted in a decrease in ROS production upon *T. cruzi* infection. Since killing of *T. cruzi* by macrophages has been associated with ONOO $^-$ (21), we suggest that impaired parasite growth in AhR KO macrophages is due to the lack of the oxidative signal that was shown to be necessary for parasite growth inside these cells (19, 47).

The absence of AhR results in increased production of IL-12 by

dendritic cells (DC) and macrophages and in an increase in numbers of these cells. Previously, we demonstrated a function for AhR in lipoxin-mediated repression of this cytokine in DC in an infection model of *T. gondii* (5). Here, higher production of IL-12 likely triggered the increased production of IFN- γ by splenocytes and higher numbers of CD3 $^+$ CD4 $^+$ IFN- γ $^+$ and CD3 $^+$ CD8 $^+$ IFN- γ $^+$ T cells at 10 dpi, resulting in a significantly increased inflammatory and immune response compared to that seen with WT mice. Surprisingly, we did not find significant differences in the size of the CD3 $^+$ CD4 $^+$ IL-17 $^+$ population in the absence of AhR. These data suggest that, in our model, AhR was not required for the differentiation of CD3 $^+$ CD4 $^+$ IL-17 $^+$ T cells. In contrast, we found a significant increase of the IL-17 level in the mRNA in AhR KO mice at 10 dpi. In this regard, it was recently reported that B cells are important sources of IL-17 during *T. cruzi* infection and that this is an AhR-independent process (48), suggesting that the increased mRNA detected in the spleen could have been derived from B cells. One interesting aspect of the immune response found in AhR KO mice concerns the Treg cell populations (CD3 $^+$ CD4 $^+$ CD25 hi Foxp3 $^+$), which were found to be equal at 10 dpi and were probably increased at 15 dpi, as inferred from the increased Foxp3 mRNA levels. Importantly, we found that expression levels of IL-10, which is a regulatory hallmark cytokine of some subpopulations of Treg cells but is also expressed by macrophages, Th2, and natural killer cells, were reduced at 15 dpi in AhR KO mice, consistently with the previously reported function of AhR as a positive regulator of the IL-10 promoter (49). These data suggest that one of the mechanisms that result in suppression of inflammation by activated AhR during *T. cruzi* infection is mediated by IL-10 transcriptional regulation. In contrast to the results of our previous study performed using *T. gondii* tachyzoite lysate (STAg) stimulation in spleen (5), the absence of AhR did not impair the expression of the SOCS2 gene in the spleen of *T. cruzi*-infected mice, strongly suggesting that SOCS2, SOCS1, and SOCS3 do not depend on AhR for positive transcriptional regulation in splenocytes during this infection. A more detailed analysis using purified spleen cell populations would clarify the role of AhR in this process.

Since the heart is a major target organ of *T. cruzi*, we examined the role of AhR in the inflammatory process of infected mice. We found that absence of AhR did not induce an intense inflammatory response in the myocardium such as was observed in the spleen. Moreover, we found that AhR KO mice displayed a reduction in myocardial inflammation and fibrosis at 15 dpi compared to WT mice. The expression of several proinflammatory cytokines (IL-12, IL-6, and TNF) was significantly increased in the heart of infected AhR KO mice. These observations suggest that, despite the reduced number of inflammatory cells in AhR KO mice, the lack of AhR in those cells induced the production of higher levels of cytokines in response to infection than was the case in WT cells. On the other hand, the reduced levels for IFN- γ observed in hearts from AhR KO mice at 10 and 15 dpi correlate with reduced migration of T cells to the myocardium or a decreased capacity of these cells to produce IFN- γ in the absence of the AhR receptor. Of note, expression of SOCS2 in the heart of infected AhR KO mice was significantly reduced, indicating that AhR is an important transcriptional regulator of SOCS2 in this organ. We previously found that SOCS2 is essential for cardiac myocyte function during *T. cruzi* infection (5). Moreover, SOCS2 expression is also increased in purified cardiac myocytes from infected mice (data not shown). Therefore, we suggest that AhR controls SOCS2 expression specifically in cardiac myocytes. On the other hand, the decreased expression of IFN- γ could also explain the reduced expression of SOCS3 found in the myocardium of infected AhR KO mice (50).

In summary, this study demonstrated the function of AhR in experimental *T. cruzi* infection. In our model, the absence of AhR results in increased resistance to infection and in a reduction in heart inflammation *in vivo*. In parallel, AhR KO also leads to a decreased SOCS2 expression in the heart and we have previously demonstrated that SOCS2 is important for protection of the myocardium and proper cardiac function during *T. cruzi* infection (5, 24). AhR functions as a regulatory molecule controlling the intensity and duration of the inflammatory immune response in the heart of *T. cruzi*-infected mice.

An interesting finding was that AhR is required for limiting the oxidative burst in splenic macrophages in infected mice. However, *in vitro*, AhR appears to be required for the initial ROS response during early infection. These opposite responses could indicate that AhR coordinates the oxidative stress response to *T. cruzi* infection in a time- and context-dependent manner. Importantly, as ROS appears to function as a growth factor for parasite replication in macrophages, the regulation of ROS by AhR appears to be an important mechanism by which AhR could influence the course of *T. cruzi* infection. Our results provide the first data regarding a role of AhR in the modulation of ROS production during experimental *T. cruzi* infection and also suggest that AhR, originally associated with dioxin response, may contribute to the development of tissue damage in Chagas disease.

ACKNOWLEDGMENTS

This work was supported by grants from Conselho Nacional de Desenvolvimento Científico e Tecnológico (CNPq) to F.S.M., D.G.S., M.M.T., M.G.-L., L.Q.V., and M.B.H.C.; by grants from Fundação de Amparo à Pesquisa do Estado de Minas Gerais (FAPEMIG) to F.S.M., L.Q.V., D.G.S., and M.M.T.; and by the program Instituto Nacional de Ciência e Tecnologia (INCT) em Dengue (Brazil) (573876/2008-8) and INCT de Processos Redox em Biomedicina-Redoxoma (573530/2008-4).

We thank Frankcineia Assis for the technical assistance, Aline Silva de

Miranda for assistance with the statistical analyses, and Thiago Cunha (University of São Paulo) for providing the anti-AhR antibody.

FUNDING INFORMATION

This work, including the efforts of Fabiana Simao Machado, was funded by CNPq (483168/2011-4). This work, including the efforts of Fabiana Simao Machado, was funded by FAPEMIG (APQ-01738-11).

The funders had no role in study design, data collection and interpretation, or the decision to submit the work for publication.

REFERENCES

- Poland AP, Glover E, Robinson JR, Nebert DW. 1974. Genetic expression of aryl hydrocarbon hydroxylase activity. Induction of monooxygenase activities and cytochrome P1-450 formation by 2,3,7,8-tetrachlorodibenzo-p-dioxin in mice genetically "nonresponsive" to other aromatic hydrocarbons. *J Biol Chem* 249:5599–5606.
- Poland A, Glover E, Kende AS. 1976. Stereospecific, high affinity binding of 2,3,7,8-tetrachlorodibenzo-p-dioxin by hepatic cytosol. Evidence that the binding species is receptor for induction of aryl hydrocarbon hydroxylase. *J Biol Chem* 251:4936–4946.
- Quintana FJ, Sherr DH. 2013. Aryl hydrocarbon receptor control of adaptive immunity. *Pharmacol Rev* 65:1148–1161. <http://dx.doi.org/10.1124/pr.113.007823>.
- Stockinger B, Di Meglio P, Gialitakis M, Duarte JH. 2014. The aryl hydrocarbon receptor: multitasking in the immune system. *Annu Rev Immunol* 32:403–432. <http://dx.doi.org/10.1146/annurev-immunol-032713-120245>.
- Machado FS, Johndrow JE, Esper L, Dias A, Bafica A, Serhan CN, Aliberti J. 2006. Anti-inflammatory actions of lipoxin A4 and aspirin-triggered lipoxin are SOCS-2 dependent. *Nat Med* 12:330–334. <http://dx.doi.org/10.1038/nm1355>.
- Stevens EA, Mezrich JD, Bradfield CA. 2009. The aryl hydrocarbon receptor: a perspective on potential roles in the immune system. *Immunology* 127: 299–311. <http://dx.doi.org/10.1111/j.1365-2567.2009.03054.x>.
- Shi LZ, Faith NG, Nakayama Y, Suresh M, Steinberg H, Czuprynski CJ. 2007. The aryl hydrocarbon receptor is required for optimal resistance to *Listeria monocytogenes* infection in mice. *J Immunol* 179:6952–6962. <http://dx.doi.org/10.4049/jimmunol.179.10.6952>.
- Sanchez Y, de Dios Rosado J, Vega L, Elizondo G, Estrada-Muñoz E, Saavedra R, Juárez I, Rodríguez-Sosa M. 2010. The unexpected role for the aryl hydrocarbon receptor on susceptibility to experimental toxoplasmosis. *J Biomed Biotechnol* 2010:505694. <http://dx.doi.org/10.1155/2010/505694>.
- Brant F, Miranda AS, Esper L, Rodrigues DH, Kangussu LM, Bonaventura D, Soriani FM, Pinho V, Souza DG, Rachid MA, Weiss LM, Tanowitz HB, Teixeira MM, Teixeira AL, Machado FS. 12 May 2014. Immune response profile and development of pathology during *Plasmodium berghei* Anka infection: the role of the aryl hydrocarbon receptor (AhR). *Infect Immun* <http://dx.doi.org/10.1128/IAI.01733-14>.
- Wheeler JL, Martin KC, Lawrence BP. 2013. Novel cellular targets of AhR underlie alterations in neutrophilic inflammation and inducible nitric oxide synthase expression during influenza virus infection. *J Immunol* 190:659–668. <http://dx.doi.org/10.4049/jimmunol.1201341>.
- Elizondo G, Rodríguez-Sosa M, Estrada-Muñoz E, Gonzalez FJ, Vega L. 2011. Deletion of the aryl hydrocarbon receptor enhances the inflammatory response to *Leishmania major* infection. *Int J Biol Sci* 7:1220–1229.
- WHO. 2014. Chagas disease (American trypanosomiasis). WHO, Geneva, Switzerland. <http://www.who.int/mediacentre/factsheets/fs340/en/>. Accessed 27 July 2014.
- Machado FS, Tanowitz HB, Ribeiro AL. 2013. Pathogenesis of Chagas cardiomyopathy: role of inflammation and oxidative stress. *J Am Heart Assoc* 2:e000539.
- Aliberti JC, Cardoso MA, Martins GA, Gazzinelli RT, Vieira LQ, Silva JS. 1996. Interleukin-12 mediates resistance to *Trypanosoma cruzi* in mice and is produced by murine macrophages in response to live trypomastigotes. *Infect Immun* 64:1961–1967.
- Silva JS, Morrissey PJ, Grabstein KH, Mohler KM, Anderson D, Reed SG. 1992. Interleukin 10 and interferon gamma regulation of experimental *Trypanosoma cruzi* infection. *J Exp Med* 175:169–174. <http://dx.doi.org/10.1084/jem.175.1.169>.
- Silva JS, Vespa GN, Cardoso MA, Aliberti JC, Cunha FQ. 1995. Tumor necrosis factor alpha mediates resistance to *Trypanosoma cruzi* infection

- in mice by inducing nitric oxide production in infected gamma interferon-activated macrophages. *Infect Immun* 63:4862–4867.
17. Torrico F, Heremans H, Rivera MT, Van Marck E, Billiau A, Carlier Y. 1991. Endogenous IFN- γ is required for resistance to acute Trypanosoma cruzi infection in mice. *J Immunol* 146:3626–3632.
 18. Silva JS, Machado FS, Martins GA. 2003. The role of nitric oxide in the pathogenesis of Chagas disease. *Front Biosci* 8:s314–s325. <http://dx.doi.org/10.2741/1012>.
 19. Paiva CN, Feijó DF, Dutra FF, Carneiro VC, Freitas GB, Alves LS, Mesquita J, Fortes GB, Figueiredo RT, Souza HS, Fantappié MR, Lannes-Vieira J, Bozza MT. 2012. Oxidative stress fuels Trypanosoma cruzi infection in mice. *J Clin Invest* 122:2531–2542. <http://dx.doi.org/10.1172/JCI58525>.
 20. Alvarez MN, Peluffo G, Piacenza L, Radi R. 2011. Intraphagosomal peroxynitrite as a macrophage-derived cytotoxin against internalized Trypanosoma cruzi: consequences for oxidative killing and role of microbial peroxiredoxins in infectivity. *J Biol Chem* 286:6627–6640. <http://dx.doi.org/10.1074/jbc.M110.167247>.
 21. Piacenza L, Peluffo G, Alvarez MN, Kelly JM, Wilkinson SR, Radi R. 2008. Peroxiredoxins play a major role in protecting Trypanosoma cruzi against macrophage- and endogenously-derived peroxynitrite. *Biochem J* 410:359–368. <http://dx.doi.org/10.1042/BJ20071138>.
 22. Boverhof DR, Tam E, Harney AS, Crawford RB, Kaminski NE, Zacharewski TR. 2004. 2,3,7,8-Tetrachlorodibenzo-p-dioxin induces suppressor of cytokine signaling 2 in murine B cells. *Mol Pharmacol* 66:1662–1670. <http://dx.doi.org/10.1124/mol.104.002915>.
 23. Delgado-Ortega M, Marc D, Dupont J, Trapp S, Berri M, Meurens F. 2013. SOCS proteins in infectious diseases of mammals. *Vet Immunol Immunopathol* 151:1–19. <http://dx.doi.org/10.1016/j.vetimm.2012.11.008>.
 24. Esper L, Roman-Campos D, Lara A, Brant F, Castro LL, Barroso A, Araujo RR, Vieira LQ, Mukherjee S, Gomes ER, Rocha NN, Ramos IP, Lisanti MP, Campos CF, Arantes RM, Guatimosim S, Weiss LM, Cruz JS, Tanowitz HB, Teixeira MM, Machado FS. 2012. Role of SOCS2 in modulating heart damage and function in a murine model of acute Chagas disease. *Am J Pathol* 181:130–140. <http://dx.doi.org/10.1016/j.ajpath.2012.03.042>.
 25. Machado FS, Martins GA, Aliberti JC, Mestriner FL, Cunha FQ, Silva JS. 2000. Trypanosoma cruzi-infected cardiomyocytes produce chemokines and cytokines that trigger potent nitric oxide-dependent trypanocidal activity. *Circulation* 102:3003–3008. <http://dx.doi.org/10.1161/01.CIR.102.24.3003>.
 26. Laucella SA, Postan M, Martin D, Hubby Fralish B, Albareda MC, Alvarez MG, Lococo B, Barbieri G, Viotti RJ, Tarleton RL. 2004. Frequency of interferon- γ -producing T cells specific for Trypanosoma cruzi inversely correlates with disease severity in chronic human Chagas disease. *J Infect Dis* 189:909–918. <http://dx.doi.org/10.1086/381682>.
 27. Faulkner K, Fridovich I. 1993. Luminol and lucigenin as detectors for O₂⁻. *Free Radic Biol Med* 15:447–451. [http://dx.doi.org/10.1016/0891-5849\(93\)90044-U](http://dx.doi.org/10.1016/0891-5849(93)90044-U).
 28. Pavanelli WR, Gutierrez FR, Mariano FS, Prado CM, Ferreira BR, Teixeira MM, Canetti C, Rossi MA, Cunha FQ, Silva JS. 2010. 5-Lipoxygenase is a key determinant of acute myocardial inflammation and mortality during Trypanosoma cruzi infection. *Microbes Infect* 12:587–597. <http://dx.doi.org/10.1016/j.micinf.2010.03.016>.
 29. Vago JP, Nogueira CR, Tavares LP, Soriani FM, Lopes F, Russo RC, Pinho V, Teixeira MM, Sousa LP. 2012. Annexin A1 modulates natural and glucocorticoid-induced resolution of inflammation by enhancing neutrophil apoptosis. *J Leukoc Biol* 92:249–258. <http://dx.doi.org/10.1189/jlb.0112008>.
 30. Green LC, Wagner DA, Glogowski J, Skipper PL, Wishnok JS, Tannenbaum SR. 1982. Analysis of nitrate, nitrite, and [15N]nitrate in biological fluids. *Anal Biochem* 126:131–138. [http://dx.doi.org/10.1016/0003-2697\(82\)90118-X](http://dx.doi.org/10.1016/0003-2697(82)90118-X).
 31. Gilliam MB, Sherman MP, Griscavage JM, Ignarro LJ. 1993. A spectrophotometric assay for nitrate using NADPH oxidation by Aspergillus nitrate reductase. *Anal Biochem* 212:359–365. <http://dx.doi.org/10.1006/abio.1993.1341>.
 32. Kooy NW, Royall JA, Ischiropoulos H, Beckman JS. 1994. Peroxynitrite-mediated oxidation of dihydrorhodamine 123. *Free Radic Biol Med* 16:149–156. [http://dx.doi.org/10.1016/0891-5849\(94\)90138-4](http://dx.doi.org/10.1016/0891-5849(94)90138-4).
 33. Kimura A, Abe H, Tsuruta S, Chiba S, Fujii-Kuriyama Y, Sekiya T, Morita R, Yoshimura A. 2014. Aryl hydrocarbon receptor protects against bacterial infection by promoting macrophage survival and reactive oxygen species production. *Int Immunol* 26:209–220. <http://dx.doi.org/10.1093/intimm/dxt067>.
 34. Novais FO, Nguyen BT, Beiting DP, Carvalho LP, Glennie ND, Passos S, Carvalho EM, Scott P. 2014. Human classical monocytes control the intracellular stage of Leishmania braziliensis by reactive oxygen species. *J Infect Dis* 209:1288–1296. <http://dx.doi.org/10.1093/infdis/jiu013>.
 35. Paiva CN, Bozza MT. 2014. Are reactive oxygen species always detrimental to pathogens? *Antioxid Redox Signal* 20:1000–1037. <http://dx.doi.org/10.1089/ars.2013.5447>.
 36. Gupta S, Dhiman M, Wen JJ, Garg NJ. 2011. ROS signalling of inflammatory cytokines during Trypanosoma cruzi infection. *Adv Parasitol* 76:153–170. <http://dx.doi.org/10.1016/B978-0-12-385895-5.00007-4>.
 37. Quintana FJ. 2013. The aryl hydrocarbon receptor: a molecular pathway for the environmental control of the immune response. *Immunology* 138:183–189. <http://dx.doi.org/10.1111/imm.12046>.
 38. Carreira VS, Fan Y, Kurita H, Wang Q, Ko CI, Naticchioni M, Jiang M, Koch S, Zhang X, Biesiada J, Medvedovic M, Xia Y, Rubinstein J, Puga A. 2015. Disruption of Ah receptor signaling during mouse development leads to abnormal cardiac structure and function in the adult. *PLoS One* 10:e0142440. <http://dx.doi.org/10.1371/journal.pone.0142440>.
 39. Görlach A, Diebold I, Schini-Kerth VB, Berchner-Pfannschmidt U, Roth U, Brandes RP, Kietzmann T, Busse R. 2001. Thrombin activates the hypoxia-inducible factor-1 signaling pathway in vascular smooth muscle cells: Role of the p22(phox)-containing NADPH oxidase. *Circ Res* 89:47–54. <http://dx.doi.org/10.1161/hh1301.092678>.
 40. Vogel CF, Khan EM, Leung PS, Gershwin ME, Chang WL, Wu D, Haarmann-Stemmann T, Hoffmann A, Denison MS. 2014. Cross-talk between aryl hydrocarbon receptor and the inflammatory response: a role for nuclear factor- κ B. *J Biol Chem* 289:1866–1875. <http://dx.doi.org/10.1074/jbc.M113.505578>.
 41. Huang H, Petkova SB, Cohen AW, Bouzahzah B, Chan J, Zhou JN, Factor SM, Weiss LM, Krishnamachary M, Mukherjee S, Wittner M, Kitsis RN, Pestell RG, Lisanti MP, Albanese C, Tanowitz HB. 2003. Activation of transcription factors AP-1 and NF- κ B in murine Chagas myocarditis. *Infect Immun* 71:2859–2867. <http://dx.doi.org/10.1128/IAI.71.5.2859-2867.2003>.
 42. Vespa GN, Cunha FQ, Silva JS. 1994. Nitric oxide is involved in control of Trypanosoma cruzi-induced parasitemia and directly kills the parasite in vitro. *Infect Immun* 62:5177–5182.
 43. Nathan C, Shiloh MU. 2000. Reactive oxygen and nitrogen intermediates in the relationship between mammalian hosts and microbial pathogens. *Proc Natl Acad Sci U S A* 97:8841–8848. <http://dx.doi.org/10.1073/pnas.97.16.8841>.
 44. Underhill DM. 2003. Macrophage recognition of zymosan particles. *J Endotoxin Res* 9:176–180. <http://dx.doi.org/10.1177/09680519030090030601>.
 45. Denison MS, Soshilov AA, He G, DeGroot DE, Zhao B. 2011. Exactly the same but different: promiscuity and diversity in the molecular mechanisms of action of the aryl hydrocarbon (dioxin) receptor. *Toxicol Sci* 124:1–22. <http://dx.doi.org/10.1093/toxsci/kfr218>.
 46. Menna-Barreto RF, de Castro SL. 2014. The double-edged sword in pathogenic trypanosomatids: the pivotal role of mitochondria in oxidative stress and bioenergetics. *Biomed Res Int* 2014:614014.
 47. Goes GR, Rocha PS, Diniz AR, Aguiar PH, Machado CR, Vieira LQ. 2016. Trypanosoma cruzi needs a signal provided by reactive oxygen species to infect macrophages. *PLoS Negl Trop Dis* 10:e0004555. <http://dx.doi.org/10.1371/journal.pntd.0004555>.
 48. Bermejo DA, Jackson SW, Gorosito-Serran M, Acosta-Rodriguez EV, Amezcua-Vesely MC, Sather BD, Singh AK, Khim S, Mucci J, Liggitt D, Campetella O, Oukka M, Gruppi A, Rawlings DJ. 2013. Trypanosoma cruzi trans-sialidase initiates a program independent of the transcription factors ROR γ t and Ahr that leads to IL-17 production by activated B cells. *Nat Immunol* 14:514–522. <http://dx.doi.org/10.1038/ni.2569>.
 49. Wagage S, John B, Krock BL, Hall AO, Randall LM, Karp CL, Simon MC, Hunter CA. 2014. The aryl hydrocarbon receptor promotes IL-10 production by NK cells. *J Immunol* 192:1661–1670. <http://dx.doi.org/10.4049/jimmunol.1300497>.
 50. Gatto L, Berlato C, Poli V, Timinini S, Kinjo I, Yoshimura A, Cassatella MA, Bazzoni F. 2004. Analysis of SOCS-3 promoter responses to interferon γ . *J Biol Chem* 279:13746–13754. <http://dx.doi.org/10.1074/jbc.M308999200>.